THERAPEUTIC ADVANCES in
Medical Oncology

Original Research

Cancer immune profiling unveils biomarkers, immunological pathways, and cell type score associated with glioblastoma patients' survival

Ther Adv Med Oncol

2022, Vol. 14: 1–15

DOI: 10.1177/17588359221127678

Daniel Antunes Moreno, Luciane Sussuchi da Silva, Isabella Gomes, Letícia Ferro Leal, Gustavo Noriz Berardinelli, Gisele Melo Gonçalves, Caio Augusto Pereira, Iara Viana Vidigal Santana, Marcus de Medeiros Matsushita, Krishna Bhat, Sean Lawler and Rui Manuel Reis

Correspondence to:
Rui Manuel Reis
Molecular Oncology Research Center, Barretos Cancer Hospital, Rua Antenor Duarte Villela, 1331, Barretos, São Paulo CEP 14784 400, Brazil

Department of Molecular Diagnosis, Barretos, São Paulo, Brazil ICVS/3B's PT Government Associate Laboratory, Braga/Guimarães, Portugal
Life and Health Sciences Research Institute (ICVS), School of Medicine, University of Minho, Braga, Portugal
ruireis.hcb@gmail.com; rreis@med.uminho.pt

Daniel Antunes Moreno
Luciane Sussuchi da Silva
Isabella Gomes
Letícia Ferro Leal
Molecular Oncology Research Center, Barretos, São Paulo, Brazil

Gustavo Noriz Berardinelli
Department of Molecular Diagnosis, Barretos, São Paulo, Brazil

Gisele Melo Gonçalves
Caio Augusto Pereira
Department of Medical Oncology, Barretos, São Paulo, Brazil

Iara Viana Vidigal Santana
Marcus de Medeiros Matsushita
Pathology Department, BCH, Barretos, São Paulo, Brazil

Krishna Bhat
Department of Translational Molecular Pathology, The University of Texas MD Anderson Cancer Center, Houston, TX, USA

Sean Lawler
Harvard Medical School, Boston, MA, USA Brown University, Pathology and Laboratory Medicine, Providence, Rhode Island, USA

Abstract

Introduction: Glioblastoma (GBM), isocitrate dehydrogenase (*IDH*) wild-type (IDH^{wt}), and grade 4 astrocytomas, *IDH* mutant (IDH^{mut}), are the most common and aggressive primary malignant brain tumors in adults. A better understanding of the tumor immune microenvironment may provide new biomarkers and therapeutic opportunities.

Objectives: We aimed to evaluate the expression profile of 730 immuno-oncology-related genes in patients with IDH^{wt} GBM and IDH^{mut} tumors and identify prognostic biomarkers and a gene signature associated with patient survival.

Methods: RNA was isolated from formalin-fixed, paraffin-embedded sections of 99 tumor specimens from patients treated with standard therapy. Gene expression profile was assessed using the Pan-Cancer Immune Profiling Panel (Nanostring Technologies, Inc., Seattle, WA, USA). Data analysis was performed using nSolverSoftware and validated in The Cancer Genome Atlas. In addition, we developed a prognostic signature using the cox regression algorithm (Least Absolute Shrinkage and Selection Operator).

Results: We found 88 upregulated genes, high immunological functions, and a high macrophage score in IDH^{wt} GBM compared to IDH^{mut} tumors. Regarding IDH^{wt} GBM, we found 24 upregulated genes in short-term survivors (STS) and overexpression of *CD274* (programmed death-ligand 1, PD-L1). Immune pathways, CD45, cytotoxic, and macrophage scores were upregulated in STS. Two different prognostic groups were found based on the 12-gene signature (CXCL14, PSEN2, TNFRSF13C, IL13RA1, MAP2K1, TNFSF14, THY1, CTSL, ITGAE, CHUK, CD207, and IFITM1).

Conclusion: The elevated expression of immune-oncology-related genes was associated with worse outcome in IDH^{wt} GBM patients. Increased immune functions, CD45, cytotoxic cells, and macrophage scores were associated with a more aggressive phenotype and may provide promising possibilities for therapy. Moreover, a 12 gene-based signature could predict patients' prognosis.

Keywords: biomarkers, glioblastoma, immune-oncology, nCounter, prognosis

Received: 30 March 2022; revised manuscript accepted: 2 September 2022.

Importance of the study

The investigation of the expression profile of 730 immune oncology-related genes in GBM by nCounter performed in the present study revealed substantial differences between *IDH* wild-type (IDH^{wt}) and *IDH* mutant tumors. Importantly, the analysis of the differences in gene expression, immunological functions, and cell type score between

short-term survivors and long-term survivors *IDH*^{wt} GBM provided important immune factors associated with tumor aggressiveness, which were further validated in public datasets. The 12-gene signature identified by the cox regression method can lead to better patient prognostication. Finally, the elevated immune functions and immune cell type score observed in short-term survivors should also offer new opportunities for therapy.

Introduction

Glioblastoma (GBM) (grade 4 glioma) is the most common primary malignant brain cancer in adults, accounting for 14.6% of all central nervous system tumors, and shows the highest mortality rate in this group.[1,2] According to the World Health Organization (WHO 2021), GBM are grade 4 diffuse astrocytic tumors wild-type for isocitrate dehydrogenase (*IDH1/2*), with one or more features: microvascular neovascularization, necrosis, +7/-10 copy number changes, *EGFR* amplification, or *TERT* promoter mutation.[2] *IDH1/2* wild-type (*IDH*^{wt}) GBM arises 'de novo', accounting for 90% of cases, affects older patients (median, 62 years), and is associated with poor prognosis, with a median overall survival (OS) of 15 months.[3] In the new 2021 classification, grade 4 astrocytomas with mutations in *IDH1/2* (*IDH*^{mut}) are no longer considered GBM.[2] These tumors arise from the progression of lower grade astrocytomas (WHO grade 2 and 3), usually affecting younger adults (median, 44 years) and exhibiting a median OS of 31 months.[3] The identification of *CDKN2A/B* co-deletion in diffuse astrocytomas is associated with a poor prognosis and leads to the classification of grade 4, independent of necrosis or microvascular proliferation.[2] Moreover, transcriptomic studies of GBM have identified different molecular subgroups: Classical (*EGFR* alterations), proneural (*PDGFRA*/*IDH1* abnormalities), and mesenchymal (*NF1* alterations).[4]

The rapid and infiltrative growth pattern of GBM cells in the brain parenchyma renders complete gross surgical resection impossible, leading to the inevitable recurrence of therapy-resistant tumor cells.[5] Standard therapy comprises the maximum tumor gross resection followed by radiation therapy and concomitant/adjuvant temozolomide (TMZ).[6] Tumor-treating fields increase patient survival and also can be employed for GBM treatment.[7] The dismal prognosis of GBM is partly due to tumor heterogeneity and the multiplicity of altered oncogenic pathways in tumor cells.[8] Importantly, some prognostic biomarkers are reported, the O6-methylguanine-DNA methyltransferase (*MGMT*) methylation status is one of the most widely used biomarkers.[9]

Despite extensive clinical studies using various agents, patient survival has not significantly improved.[5] In recent years, many studies have demonstrated that understanding the tumor microenvironment (TME) and the immunological factors involved in tumor development and progression may provide promising and new possibilities for immunotherapy. These approaches include cancer vaccines, oncolytic viruses, chimeric antigen receptor T cells, and immune checkpoint blockade.[8]

Immunotherapy has revolutionized the treatment of some cancer types in recent years. However, so far, immunotherapies seem to have limited efficacy for brain tumors.[10] This is probably associated with the malignant cell heterogeneity, the immunosuppressive microenvironment, and the challenges of efficient drug access across the blood–brain barrier.[10]

Infiltrating immune cells in gliomas, such as lymphocytes, microglia, and tumor-associated macrophages (TAMs), may comprise more than 30% of the tumor mass and have an important role in immunosuppression, tumor development, and progression.[11] The study of the GBM immune microenvironment may provide new therapeutic concepts and lead to the discovery of novel prognostic and treatment-responsive biomarkers.

In the current survey, we evaluated the expression profile of 730 immune-oncology-related genes using the Pan-Cancer Immune Profiling Panel (NanoString Technologies, Inc., Seattle, WA, USA) in 99 samples from patients diagnosed with *IDH*^{wt} GBM and grade 4 astrocytoma *IDH*^{mut}, treated with standard of care. We evaluated the differences in gene expression profiles, immune pathways, and cell type scores between *IDH*^{wt} GBM *versus IDH*^{mut} (grade 4 astrocytoma, *IDH* mutant), and its association with the patient's survival. We found that elevated expression of immune-oncology-related genes was associated with poor survival and identified a 12-gene prognostic signature.

Materials and methods

Selection of GBM cases

We included 86 *IDH*^{wt} GBM and 13 grade 4 astrocytoma, *IDH*^{mut} specimens diagnosed at Barretos

Cancer Hospital (BCH), Barretos, Brazil, from 2009 to 2018 and treated according to the standard therapy protocol: surgery, radiotherapy, and concomitant/adjuvant TMZ-based chemotherapy and with available formalin-fixed, paraffin-embedded (FFPE) samples for molecular analysis. Tumor specimens were reviewed by two experienced neuropathologists. These patients were previously characterized molecularly for *IDH1* mutation status, ATRX expression, *TERT* promoter mutations, and *MGMT* methylation.[9] The clinicopathological and molecular features are summarized in Supplemental Table 1. The 13 grade 4 astrocytomas, IDH mutant included in the present study, showed microvascular proliferation, necrosis, and *IDH1*^{R132H} mutation. *IDH2* mutations and *CDKN2A/B* codeletion were not evaluated. This study was approved by the institutional review board (IRB) from BCH (IRB 1604/2018).

Microsatellite instability analysis

Microsatellite instability (MSI) evaluation was performed using a multiplex polymerase chain reaction (PCR; Qiagen Multiplex Kit, Venlo, The Netherlands) comprising the following six quasi-monomorphic mononucleotide repeat markers: BAT-25, BAT-26, NR- 21, NR-24, NR-27, and HSP110.[12] PCR was performed using 0.5 µL of DNA at 50 ng/mL using reverse primers end-labeled with fluorescent dyes as previously described.[12] The quasimonomorphic variation range of each marker was established from an average of the allele size with a range of ±3 nucleotides.[12,13]

RNA and DNA isolation

Nucleic acid isolation was performed from macrodissected FFPE GBM as reported.[9] The tumor area was previously marked by an experienced pathologist, ensuring the presence of >80% of tumor cells and the absence of microvascular proliferation and necrosis. DNA isolation was performed using the QIAamp DNA Mini Kit (Qiagen, Venlo, The Netherlands), and NanoDropVR 2000 (Thermo Scientific, Waltham, MA, USA) was used for DNA quantification according to the manufacturer's instructions.

RNA isolation was performed using the RNeasy Mini Kit (Qiagen, Venlo, The Netherlands), and the Qubit 2.0 Fluorometer (RNA HS Assay kit, Life Technologies, Thermo Fisher Scientific, Waltham, MA USA) was applied for RNA quantification following the manufacturer's recommendations.

Gene expression experiments

Gene expression assays were performed in the nCounter® FLEX Analysis System available in the Molecular Oncology Research Center of BCH using the nCounter® Pan-Cancer Immune Profiling Panel (NanoString Technologies, Inc.). This panel comprises 40 reference genes and 730 immuno-oncology-related targets, including 109 cell surface markers for 14 immune cell types[14] (Supplemental Table 2). The complete list of the Pan-Cancer Immune Profiling Panel is available at https://www.nanostring.com/products/ncounter-assays-panels/oncology/pancancer-immune-profiling/.

The NanoString assays were performed using 150 ng of RNA, 5 µL of hybridization buffer, 3 µL of reporter probe, and 2 µL of capture probe per sample. The hybridization reaction was performed for 24 h at 65°C in a thermocycler (Proflex™ PCR System, Applied Biosystems, Foster City, CA, USA). Cartridge scanning was performed with 555 fields of view in the nCounter® Digital Analyzer (NanoString Technologies, Seattle, WA, USA).

NanoString data analysis

The nSolver™ Analysis Software v4.0 (NanoString Technologies®) was applied to evaluate quality control parameters such as binding density, the limit of detection, and positive controls. In addition, the raw data were evaluated in the R statistical environment (version 3.6.3) with the Quantro package (version 1.18.0) to guide the normalization process. No quality control flags were detected, and all 99 samples were included in further analysis. Housekeeping selection, normalization, differential expression, and immune-oncology-related scores calculation were performed in the Advanced Analysis module from the nSolver™ Analysis Software v4.0 (NanoString Technologies®).

The geNorm algorithm implemented in the advanced analysis module was used for the automatic selection of the housekeeping genes for data normalization. The cutoff to consider differentially expressed genes was the adjusted p value less than 0.1. Further statistical analyses of the pathway and cell type scores were performed

using the nonparametric Mann–Whitney test for independent samples (IBM SPSS 2.3 version).

Pathway images were generated using the Kyoto Encyclopedia of Genes and Genomes (KEGG), available in the nSolver Advanced Analysis module. Normalized data of differentially gene expression data were downloaded from the nSolver software for survival analysis of *IDH*^{wt} GBM.

Analysis of differentially expressed immune-oncology genes in IDH^{wt} *GBM and survival in public databases*

To evaluate the association between OS and median mRNA expression for GBM patients from The Cancer Genome Atlas (TCGA) dataset, we used the cBioPortal (RNAseq: Legacy 2013 and Harmonized 2018) (https://www.cbioportal.org/) and the Betastasis (microarray: Affymetrix HT HG U133A and Human Exon 1.0 ST) (http://www.betastasis.com/) webservers. The differentially expressed genes identified for the *IDH*^{wt} GBM STS group were evaluated in the public databases, with the median expression was applied to split groups for the Kaplan–Meier curves (log-rank test). The null hypothesis was rejected when $p < 0.05$.

Analysis of differentially expressed immune checkpoints genes in IDH^{wt} *GBM*

We analyze five major immune checkpoint-related genes *PDCD1* (PD-1), *CD274* (PD-L1), *CTLA4*, *IDOL1*, and *LAG3* in *IDH*^{wt} GBM STS and LTS. The Mann–Whitney nonparametric test (SPSS IBM software) was applied to evaluate the possible differences using the normalized mRNA counts. Significant differences were considered when $p < 0.05$.

Establishment of a prognostic signature for IDH^{wt} *GBM*

Normalized data from nSolver analysis of the 86 *IDH*^{wt} GBM samples were applied to define a prognostic signature based on the nCounter® Pan-Cancer Pathways Panel using the R statistical environment (version 3.6.3). First, univariate analyses were performed to select genes significantly associated with survival (Survival package, version 3.2-7). The selected genes were applied in the Least Absolute Shrinkage and Selection Operator (LASSO) regression with Cox proportional hazards model using the glmnet package (version 4.1).[15] Leave-one-out cross-validation was carried out to select the λ value with minimum mean cross-validated error (λ_{min}). The risk score based on the coefficients of the regression was calculated and used to classify the patients into low- and high-risk groups using the median value of the risk scores. Kaplan–Meier curves were built with the survminer package (version 0.4.8), and time-dependent ROC (receiver operator characteristic) curves were built with the timeROC package (version 0.4). C-indexes were calculated using the suvcomp package (version 1.34.0).

Results

Clinical and molecular characteristics of GBM patients

The clinical and molecular data from GBM patients included in the present study ($n = 99$) were recently reported in a larger cohort.[9] The frequencies of the clinical and molecular features of the GBM cohort included in the present study are summarized in Supplemental Table 1.

The 86 *IDH1*^{wt} GBM patients showed a median OS of 15.87 months and a progression-free survival (PFS) of 7.83 months (Supplemental Figures 1(a) and (b)). The 13 grade 4 astrocytomas *IDH*^{mut} (13.1%) patients showed a median OS of 35.45 months and a PFS of 18.13 months (Supplemental Figures 1(c) and (d)). Total surgical resection ($p = 0.004159$), age less than 40 years ($p = 0.028151$), *MGMT* methylation ($p = 0.000010$), and high *MGMT* mRNA expression (0.000024) were associated with higher OS (Supplemental Table 3; Supplemental Figure 2).

Since MSI is currently an agnostic marker of immunotherapy decision-making, and some studies, including our group[16], showed its presence in GBM, we performed molecular analysis for MSI. The MSI status was conclusive in 90 cases, and all cases showed no MSI (Supplemental Table 1).

Differentially expressed genes in IDH^{wt} *GBM compared to* IDH^{mut} *grade 4 astrocytoma*

We initially compared the expression of the immune-oncology-related gene panel in *IDH*^{wt} GBM ($n = 86$) *versus* *IDH*^{mut} ($n = 13$). The heatmap of normalized data generated *via* unsupervised clustering of the two groups (Figure 1(a))

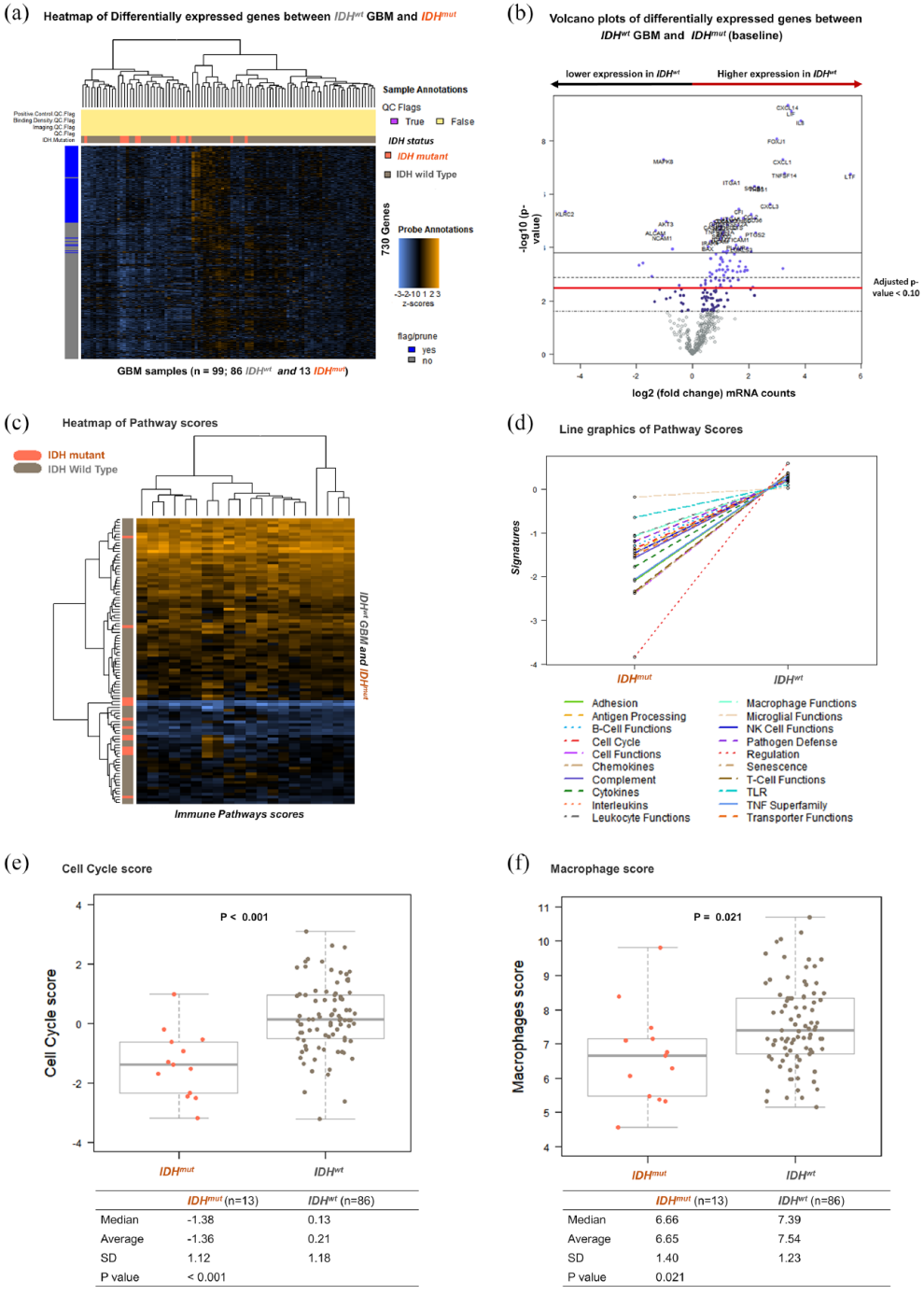

	IDHmut (n=13)	IDHwt (n=86)
Median	-1.38	0.13
Average	-1.36	0.21
SD	1.12	1.18
P value	< 0.001	

	IDHmut (n=13)	IDHwt (n=86)
Median	6.66	7.39
Average	6.65	7.54
SD	1.40	1.23
P value	0.021	

Figure 1. DE genes, pathways, and cell type scores in *IDH*^{wt} GBM ($n = 86$) and grade 4 astrocytoma *IDH*^{mut} ($n = 13$). (a) Heatmap of normalized gene expression data generated *via* unsupervised clustering. The first four horizontal bars show the positive control: QC, binding density QC, imaging QC, and QC flags. Yellow means no QC flags. The orange bar and gray bar indicate the grade 4 astrocytomas, *IDH*^{mut}, and *IDH*^{wt} GBM samples, respectively. Inside the heatmap, the box, yellow squares indicate high mRNA expression, and blue indicates low expression. (b) Volcano plot displaying each gene's –log10(p-value) and log2 fold change in *IDH*^{wt} GBM compared to *IDH*^{mut} tumors (baseline). DE genes with high statistical significance are shown from the bottom to the top. The threshold is indicated for the horizontal red line (adjusted $p < 0.10$). The more the left, the lower the expression, and the more the right, the greater the gene expression in *IDH*^{wt} GBM compared to *IDH*^{mut} tumors. (c) The heatmap of pathway scores orange indicates a high score and blue low scores. The vertical bar on the left indicates the GBM samples *IDH*^{wt} in gray and *IDH*^{mut} in orange. (d) Line graphics show each pathway's average score across values between *IDH*^{wt} and *IDH*^{mut}. (e) Cell cycle pathway score upregulated in *IDH*^{wt} GBM compared to *IDH*^{mut} tumors. (f) Macrophage score based on the higher and correlated mRNA expression of macrophage markers in *IDH*^{wt} GBM compared to *IDH*^{mut} tumors. Mann–Whitney test was applied for statistical analysis ($p < 0.05$).
DE, differentially expressed; GBM, glioblastoma; IDH, isocitrate dehydrogenase; QC, quality control.

and the Volcano plots showed the differentially expressed genes in *IDH*^{wt} GBM compared to *IDH*^{mut} (Figure 1(b)). We found 97 significant differentially expressed genes, 88 upregulated, and nine downregulated in *IDH*^{wt} GBM compared with *IDH*^{mut} (Supplemental Table 4).

Immunological functions are upregulated in IDH^{wt} *GBM compared to grade 4 astrocytoma,* IDH^{mut}

The differentially expressed genes were further evaluated by their specific immune pathways. Apart from microglial and toll-like receptor (TLR) functions, all other immune functions were upregulated in *IDH*^{wt} GBM compared to *IDH*^{mut} (Figure 1 (c) and (d)); (Supplemental Table 5). The most significantly upregulated pathway score in *IDH*^{wt} GBM compared to *IDH*^{mut} was the cell cycle score ($p < 0.01$) (Figure 1(e)). Moreover, the analysis of the cell type score showed the high macrophage score in *IDH*^{wt} GBM compared to *IDH*^{mut} tumors ($p = 0.021$) (Figure 1(f)).

Using the KEGG, we analyzed the pathways in cancer and found that the VEGF, TGFB, interleukin (IL)-8, COX-2, cytokine receptor, and ITGA are upregulated in *IDH*^{wt} GBM (yellow nodes) compared to *IDH*^{mut} tumors (Supplemental Figure 3).

High expression of immuno-oncology genes in IDH^{wt} *GBM was observed in short-term survivors*

Based on the patient's OS, we further divided the *IDH*^{wt} GBM patients into short-term survivors (STS, less than 1 year) and long-term survivors (LTS, more than 3 years). This led to 26 STS (median OS = 7.95 months) and 11 LTS (median OS = 42.94 months) patients.

Comparisons of differentially expressed genes between both groups showed overexpression of immune-oncology-related genes in STS (Figures 2(a) and (b)). In all, 24 genes were overexpressed, and two were downregulated in STS compared with LTS (Table 1). Kaplan–Meier analysis also showed significant differences in OS in 20 of 24 of the differentially expressed genes in *IDH*^{wt} GBM STS and LTS groups. Except for *MARCO, TGFB2, TFEB*, and *CCND3*, all other 20 differentially expressed genes were also correlated with median OS in our cohort ($n = 86$) (Table 1). The 24 differentially expressed genes were further analyzed in the TCGA database. These analyses showed that 18 of 24 genes were significantly associated with GBM survival in at least one TCGA dataset (Table 1).

In addition, the immune pathway scores were also associated with *IDH*^{wt} GBM survival (Figures 2(c) and (d); Supplemental Table 6). Except for TLR, microglial, and cell cycle pathway scores, all other immune pathways were upregulated in *IDH*^{wt} GBM STS. The most significant upregulated pathway in STS was macrophage functions (Supplemental Table 6; Figure 2(e)). We also observed significant upregulation of macrophages (Figure 2(f)), CD45 (Figure 2(g)), and cytotoxic cell type score (Figure 2(h)) in STS compared to LTS.

KEGG pathway analysis showed upregulation of SDF1, cytokine receptors, IL8, TGFB, and downregulation of Cyclin D pathways *IDH*^{wt} GBM STS (Supplemental Figure 4).

CD274 (PD-L1) immune checkpoint mRNA is overexpressed in short-term survival IDHwt GBM.

We also evaluated the expression profile of important immunotherapy genes related to T-cell exhaustion. We observed a high expression of *CD274* (PD-L1) in *IDH*^{wt} GBM STS ($p = 0.009$) compared to LTS. No significant differences were observed for *PDCD1* (PD-1), *CTLA4, IDO1*, and *LAG3*. The nSolver software analysis also showed that *CD274* is upregulated in STS (Log2 fold change = 1.22; $p = 0.015$). However, the adjusted p-value observed for this analysis was 0.45.

The immune-oncology signature predicts prognosis in GBM IDH^{wt}

To identify a prognostic *IDH*^{wt} GBM gene signature, we initially performed a univariate analysis of the 730 immune-oncology genes included in the NanoString Pan-Cancer Immune Profiling Panel. We found 280 genes with significant association with patient survival that were further submitted to the LASSO regression with Cox proportional hazards model (Supplemental Table 7). From leave-one-out cross-validation, λ_{min} was automatically selected to define the prognostic signature. We obtained a 12-gene signature (*CXCL14, PSEN2, TNFRSF13C, IL13RA1, MAP2K1, TNFSF14, THY1, CTSL, ITGAE, CHUK,*

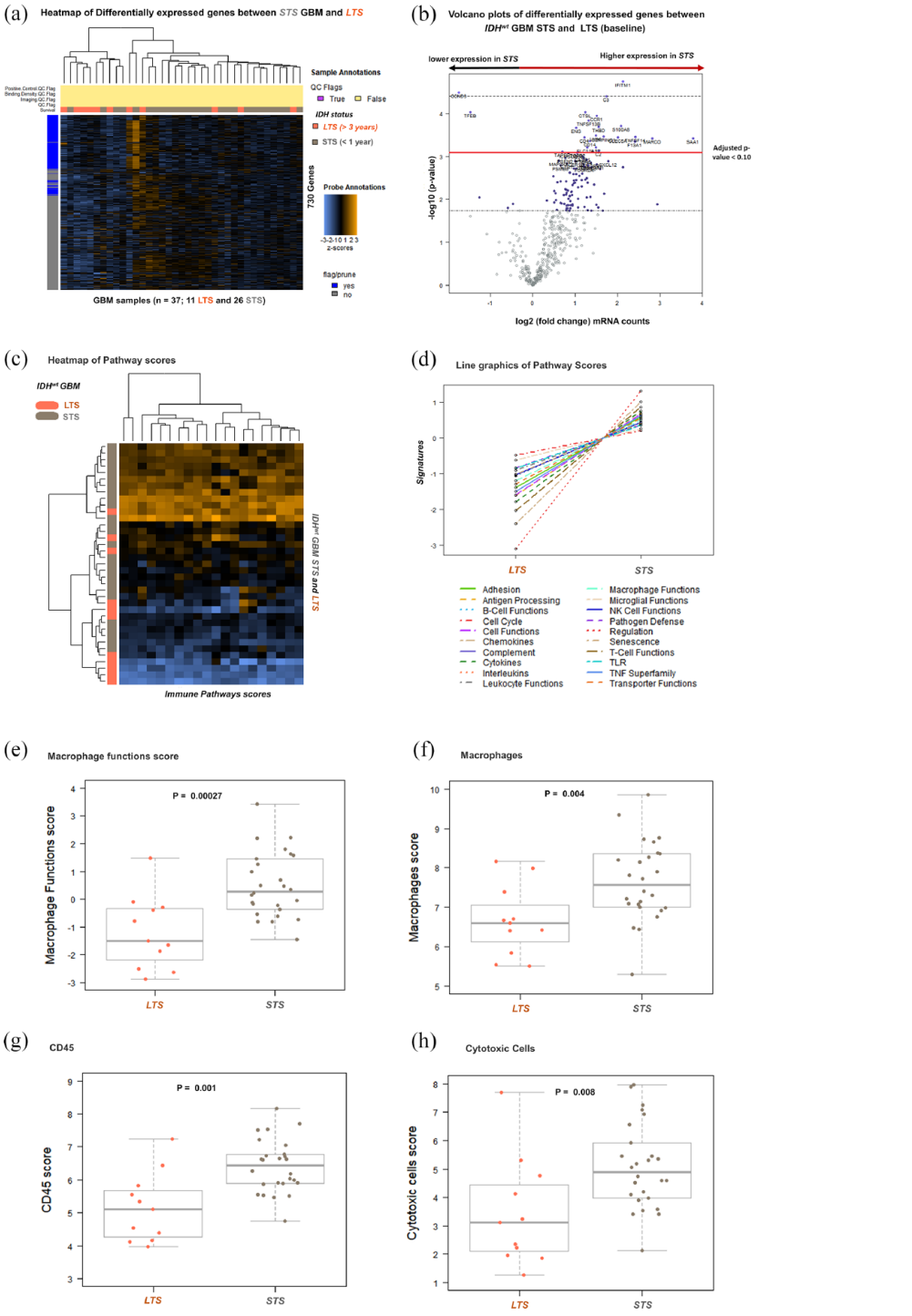

Figure 2. DE genes, pathways scores, and cell type scores in *IDH*^{wt} GBM LTS and STS. (a) Heatmap of normalized gene expression data generated *via* unsupervised clustering. In orange are represented the LTS ($n = 11$), and in gray, the STS ($n = 26$). (b) Volcano plot displaying each gene's –log10 (p-value) and log2 fold change in STS compared to LTS (baseline). Genes on the right and above the red line (adjusted $p < 0.1$) are upregulated in STS ($n = 24$), and genes above the red line on the left are downregulated in STS. (c) The heatmap of pathway scores. Yellow squares indicate a high pathway score, and blue indicates a low pathway score. The vertical bar on the left indicates the GBM samples. The 26 STS are marked in grey, and the 11 LTS in orange. (d) Line graphics show each pathway's average score across values between LTS and STS. (e) The macrophage functions score. (f) Macrophages score. (g) CD45 score. (h) Cytotoxic cells score.
GBM, glioblastoma; DE, differentially expressed; GBM, glioblastoma; LTS, long-term survivors; STS, short-term survivors.

Table 1. Description of *IDH*^{wt} GBM survival-associated genes found with the nanostring Pan-Cancer Immune Profiling Panel and survival evaluation using public databases.

DE genes in *IDH*^{wt} GBM	Nanostring (STS *versus* LTS) BCH 2021 Log2FC (*p*-value) (*n* = 37)	Nanostring (Kaplan–Meier) BCH 2021 (*n* = 86)	cBioPortal legacy 2013 GBM (*n* = 151)	cBioPortal harmonized 2018 GBM (*n* = 154)	Betastasis affymetrix human exon 1.0 ST (*n* = 454)	Betastasis affymetrix HT HG U133A (*n* = 453)
Upregulated						
SAA1	3.78 (**0.00038**)	**0.00034**	*0.053*	**0.018**	0.132	0.234
MARCO	2.82 (**0.00038**)	0.055	**0.044**	*0.059*	0.692	0.248
TNFSF14	2.42 (**0.000348**)	**0.012**	**0.0013**	**0.0039**	*0.150*	0.637
F13A1	2.41 (**0.000449**)	**0.0067**	0.32	0.18	***0.0328***	**0.0474**
IFITM1	2.13 (**1.8e–05**)	<**0.0001**	0.56	0.36	0.710	0.411
S100A8	2.09 (**0.000192**)	**0.00056**	0.29	0.2	**0.0142**	0.0613
CLEC5A	2.01 (**0.000358**)	**0.0041**	0.061	0.16	0.114	**0.00199**
C3	1.74 (**3.88e–05**)	**0.00072**	0.66	0.96	*NF*	*NF*
SERPING1	1.67 (**0.000339**)	**0.0018**	0.074	0.15	*0.0661*	**0.0442**
C2	1.56 (**0.000735**)	**0.0017**	0.075	0.82	0.397	0.300
THBD	1.55 (**0.000202**)	**0.0028**	**0.019**	0.16	**0.0481**	*NF*
CCR1	1.51 (**0.000113**)	**0.00063**	0.18	0.89	0.220	0.302
LY96	1.49 (**0.000328**)	**0.00059**	**0.044**	*0.069*	**0.00506**	**0.0132**
IL32	1.49 (**0.000614**)	**0.00042**	0.31	0.34	0.747	*NF*
CD14	1.35 (**0.000434**)	**0.00043**	0,27	0,18	**0.0243**	*0.0517*
TNFSF13B	1,32 (**0.000145**)	**0.011**	0,084	0,11	**0.0133**	*NF*
SLC11A1	1,28 (**0.000612**)	**0.00013**	**0,011**	0,14	0.0999	**0.00564**
CTSL	1.24 (**9.25e–05**)	<**0.0001**	**0,033**	**0.013**	**0.0124**	**0.00893**
CD4	1.22 (**0.000355**)	**0.0042**	0.077	0.88	0.157	0.105
TGFB2	1.06 (**0.000788**)	0.28	0.85	0.93	0.516	0.367
CD68	1.05 (**0.000825**)	**0.00016**	**0.047**	0.23	0.124	0.108
ENG	1.02 (**0.000215**)	**0.00048**	0.68	0.94	**0.0103**	0.307
ICOSLG	0.84 (**0.000832**)	**0.0028**	0.16	0.18	0.599	0.772
TAPBP	0.7 (**0.000774**)	**0.0039**	0.094	**0.0047**	0.367	*NF*
Downregulated						
TFEB	–1.47 (**9.23e–05**)	0.44	0.893	0.920	**0.0191**	0.391
CCND3	–1.75 (**3.2e–05**)	0.65	0.841	0.278	0.126	**0.00484**

Genes in bold: upregulated in STS. Genes in italic and underlines: downregulated in STS.
BCH, Barretos Cancer Hospital; DE, differentially expressed; GBM, glioblastoma; LTS, long-term survivors; NF, not found; OS, overall survival; STS, short-term survivors.

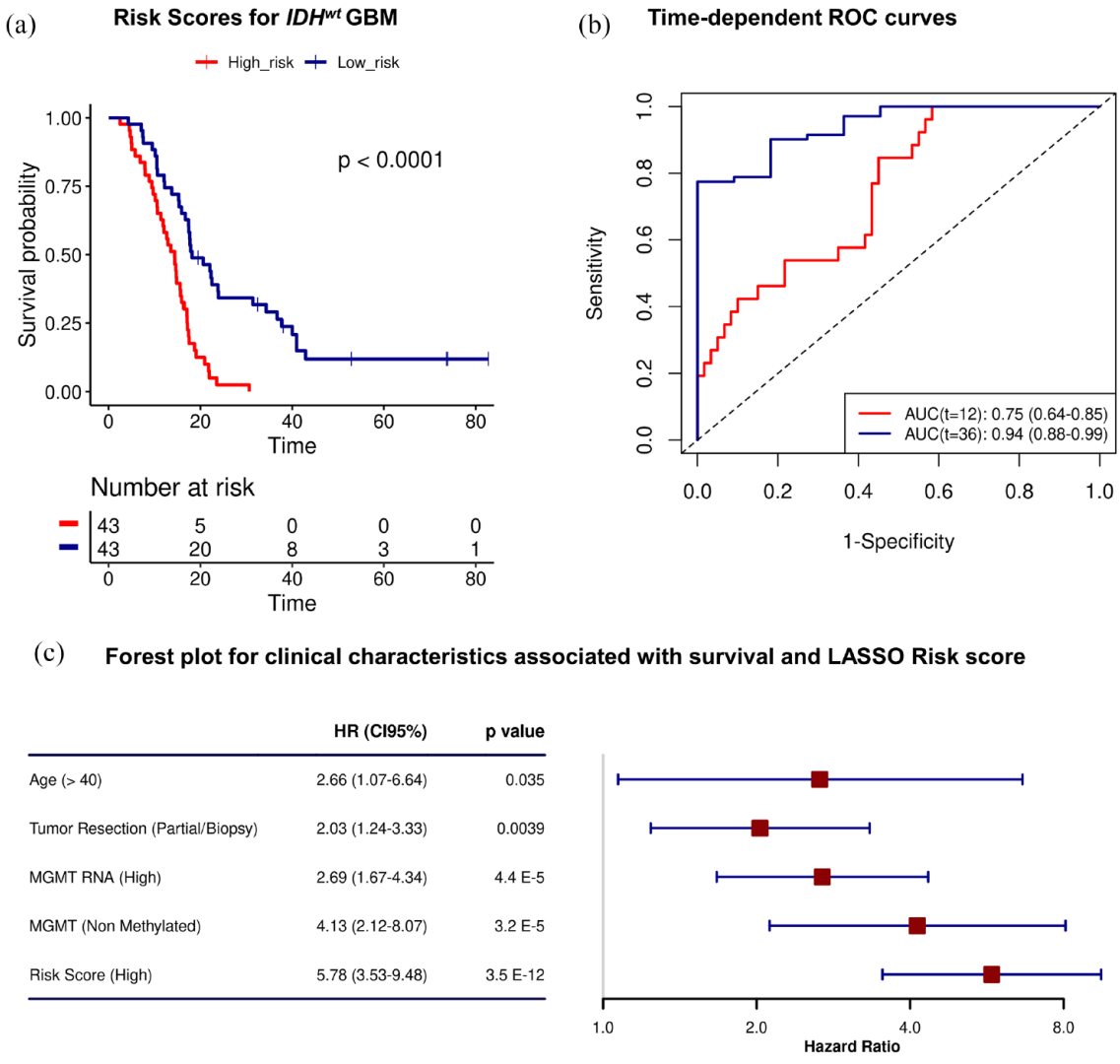

Figure 3. Performance of the 12 immune-related gene signature for *IDH*^{wt} GBM developed by LASSO regression with Cox proportional hazards model. (a) Kaplan–Meier curves based on the prognostic 12 immune-related gene signature for GBM *IDH*^{wt}. High- and low-risk groups were defined by the median risk scores. (b) Time-dependent ROC curves were built for 12 and 36 months. AUC: area under the curve. (c) Forest plot for clinical characteristics associated with GBM *IDH*^{wt} patient's survival and the LASSO risk score.
GBM, glioblastoma; IDH, isocitrate dehydrogenase; LASSO, Least Absolute Shrinkage and Selection Operator.

CD207, and *IFITM1*) with active non-zero coefficients were obtained (Supplemental Table 8).

The 12 immune-related gene signature score for *IDH*^{wt} GBM was evaluated using Kaplan–Meier analysis (Figure 3(a)) and the time-dependent ROC curves for patient survival (Figure 3(b)). Low- and high-risk patients were defined by a median value of the signature score, which presented a median OS of 18.17 (16.69–31.44) and 14.36 (11.37–16.46) months, respectively. The estimated area under the curve for 12 and 36 months were 0.75 and 0.94, respectively (Figure 3(b)). A general C-index of 0.72 was obtained for the model cohort.

In addition, the 12 immune-related gene prognostic signature showed a higher risk score (Hazard Ratio, HR = 5.78) compared to other clinical and molecular prognostic characteristics in *IDH*^{wt} GBM such as age >40 (HR = 2.66); partial/biopsy tumor resection (HR = 2.03); *MGMT* high expression by Nanostring (HR = 2.69); and *MGMT* non-methylated (HR = 4.13) (Figure 3(c)).

This analysis underscores the importance of immune factors in GBM progression, revealing targets and biomarkers for further study.

Discussion

In the current study, we evaluated the mRNA levels of 730 immune-oncology-related genes in FFPE tissue from 86 IDH^{wt} GBM and 13 grade 4 astrocytomas IDH^{mut} using the nanostring Pan-Cancer Immune Profiling Platform. We investigated the differences in the immune profiles between the GBM IDH^{wt} and grade 4 astrocytomas IDH^{mut}. We further analyzed the differences in the immune profiles between STS and LTS in IDH^{wt} GBM, identifying immune-related biomarkers and putative targets for GBM therapy.

Immunotherapy of primary brain tumors, particularly GBM, has not been successful despite the notable successes in other solid tumors.[10] This may be due to various features, such as low mutation burden, the highly immunosuppressed brain microenvironment, protection by the blood–brain barrier, and differences in immune cell infiltrates compared with other body locations.[10] Therefore, a better understanding of the immune factors associated with GBM is needed to develop new therapeutic strategies and identify novel biomarkers.

Comparing the expression profile between IDH^{wt} GBM and IDH^{mut} grade 4 astrocytomas, the lactotransferrin (*LTF*) gene was the most upregulated gene in IDH^{wt} GBM. According to our findings, the *LTF* gene was downregulated in the pro-neural GBM transcriptional subtype[17], which is also associated with IDH^{mut} tumors.[18] Another differentially expressed gene in GBM IDH^{wt} compared with IDH^{mut} was the pro-inflammatory cytokine IL8, which was reported to be associated with more aggressive gliomas.[19] The third most differentially expressed gene in IDH^{wt} GBM was leukemia inhibitory factor (*LIF*). LIF is a cytokine involved in multiple biologic processes, and its expression in gliomas was reported to prevent differentiation and to induce self-renewal of glioma-initiating cells.[20] Moreover, among the 10 most upregulated genes in IDH^{wt} GBM compared to IDH^{mut} tumors, we found three different chemokines (C-X-C motif) ligands (*CXCL14*, *CXCL1*, and *CXCL3*). These results agree with previous studies that showed chemokine (C-X-C motif) ligands are downregulated in IDH^{mut} gliomas, and it can be due to 2 hydroxybutyrate, a product that accumulates in glioma cells as a result of the enzymic activity of mutated IDH1/2.[10]

The most upregulated immune pathway observed in IDH^{wt} GBM was the cell cycle score, which may be related to the more aggressive phenotype of this subtype. We also observed a significantly higher macrophage cell type score in IDH^{wt} GBM compared to IDH^{mut}, corroborating other studies that reported high levels of GBM-associated macrophages in IDH^{wt} GBM compared to IDH^{mut}.[21] This pronounced difference in the immune microenvironment between IDH^{wt} GBM and IDH^{mut} grade 4 astrocytomas reflects the different etiology of these tumors, which are also genetically distinct[2] and may provide clues for future immunotherapy strategies. Nevertheless, the lower number of IDH^{mut} ($n = 13$) evaluated hampers meaningful statistical associations, and further studies with a higher number of cases should be performed.

Next, in the GBM IDH^{wt} subset, we further interrogated the immune-oncology-related genes associated with patient OS, stratifying our cohort in STS, OS less than 1 year, and LTS, OS higher than 3 years. We found 24 upregulated and two downregulated genes in STS compared with LTS (Figure 4).

Interestingly, the two most upregulated genes (*SAA1* and *MARCO*) in STS are associated with the tumor-promoting M2 macrophage subtype. It was reported that human Serum Amyloid A1 (*SAA1*) induces the expression of macrophage M2 markers[22] and contributes to M2 macrophage polarization.[23] Corroborating our data, *SAA1* overexpression was previously associated with poor outcomes in GBM[24] and is a promising target for future GBM therapy. High levels of macrophage receptor with collagenous structure (*MARCO*) were also reported to be associated with the immunosuppressive M2 macrophage signature.[25] Moreover, a recent study demonstrated that the *MARCO* overexpression in TAMs drives the malignant phenotype in GBM.[26] Additional anti-inflammatory M2 macrophage biomarkers overexpressed in the GBM IDH^{wt} STS group were *CLEC5A* and cathepsin L (*CTSL*). In agreement with our findings, a recent large-scale study showed that *CLEC5A* overexpression is associated with decreased OS in gliomas[27], and the proteolytic enzyme CTSL was reported to promote migration and invasion in gliomas (Figure 4).[28]

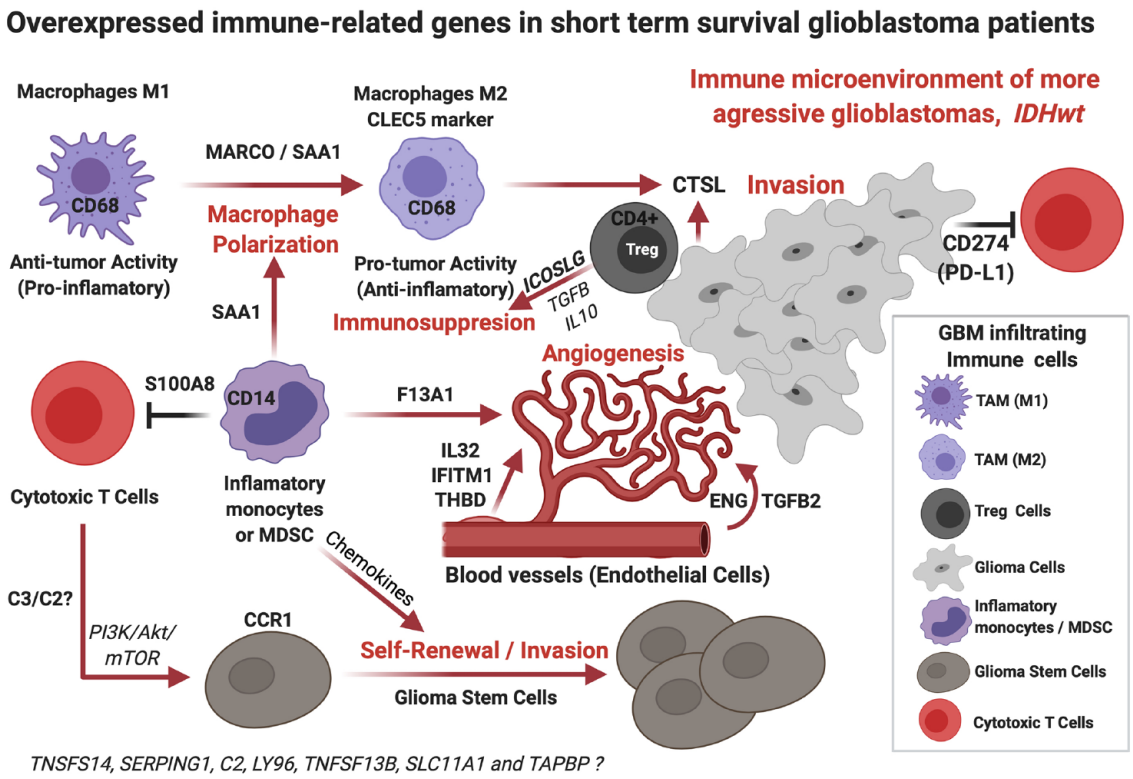

Figure 4. Schematic representation of overexpressed immune-related mRNA in short-term survival compared with long-term *IDH*^{wt} GBM. Upregulation of *MARCO* and *SAA1* secreted by inflammatory monocytes or MDSC contributes to macrophage polarization (M1 to M2). Macrophage M2 (markers *CD68* and *CLEC5*) induces immunosuppression and invasion by releasing CTSL. Treg cells also induce immunosuppression by releasing *ICOSLG*. MDSC (CD14+) produces *F13A1* stimulating angiogenesis and S100A8 attenuating the cytotoxic T-cell antitumor activity. The higher levels of C3 and C2 produced by cytotoxic T cells and *CCR1* produced in glioma stem cells may contribute to glioma stem cells' self-renewal and invasion. Endothelial TME cells produce *IL32, IFIM1, THBD, ENG*, and *TGFB2*, inducing angiogenesis.
CTSL, cathepsin L; GBM, glioblastoma; MDSC, myeloid-derived suppressor cells; TME, tumor microenvironment.

F13A1, which encodes the coagulation factor XIII, which plays functions in tissue healing and angiogenesis, was another significantly overexpressed gene in the STS group. The F13A1 contributes to neovascularization.[29] Interestingly, F13A1 was shown to be highly expressed by inflammatory monocytes in the lung cancer microenvironment, and the classical marker for inflammatory monocytes is CD14[30], which we also found to be upregulated in our STS GBM group. Other genes associated with angiogenesis, such as *IL32*[31], *IFITM1*[32], *THBD*[33], *ENG*[34], and *TGFβ2*[35], are upregulated in the GBM *IDH*^{wt} STS group (Figure 4).

We also observed overexpression of tumor necrosis factor (TNF) superfamily (TNFSF) *TNFSF14* and *TNFSF13B* in STS GBM, supporting previous studies that associated these genes with shorter survival[36] and GBM aggressiveness.[37]

Another overexpressed gene in the STS group was *S100A8*. The S100A8/A9 heterodimer is a chemoattractant for myeloid-derived suppressor cells (CD14+), which function in the tumor immunosuppressive microenvironment by suppressing T-cell function[38], and herein, we also found a significantly increased level of the MDSC marker *CD14* in STS GBM (Table 1 and Figure 4).

Interestingly, we observed upregulation of genes related to the self-renewal of glioma stem cells and invasion, such as *CCR1* that together with *CCR5* are the main receptors that mediate *CCL8* expression in TAMs contributing to invasion and stemness in GBM[39]

The complement system plays an important role in glioma stem cell maintenance and self-renewal.[40] T cells contain intracellular C3 (Complement 3), which induces activation of the PI3K/Akt/mTOR signaling cascade leading to self-renewal and maintenance of glioma stem cells.[40] In the present study, we found higher C3 and C2 in STS *IDH*^{wt} GBM (Figure 4). Furthermore, we observed upregulation of *SERPING1* (Serine/Cysteine Proteinase Inhibitor Clade G Member 1) in STS. SERPING1 is a C1-Inhibitor produced mainly by monocytes and macrophages and acts by inhibition of the classic complement system pathway.[41] However, the exact mechanisms involved in GBM aggressiveness are not well described.

We found that *CD4* is upregulated in STS *IDH*^{wt} GBM patients. CD4 is a classical surface marker of T-helper cells, induced T regulatory cells (iTreg), and T regulatory cells (Treg).[42] Tumor-associated Treg cells express the inducible costimulator (ICOS), and the expansion of these immunosuppressive cells also depends on the expression of the inducible T-cell ICOS ligand (ICOSLG) provided by dendritic cells.[43] Interestingly, we found *ICOSLG* overexpression in *IDH*^{wt} GBM STS, indicating that this may be an important factor, which may contribute to GBM immunosuppression and aggressiveness. Of note, *ICOSLG* overexpression was associated with poor prognosis in GBM, and the knockdown of *ICOSLG* reduced GBM growth in immunocompetent mice.[44]

The *TAPBP* gene encodes tapasin, part of a peptide complex, and interacts with major histocompatibility complex class I (MHC I), allowing high-affinity peptide binding for CD8+ T-cell antigen recognition.[45] Intriguingly, we observed the upregulation of *TAPBP* in *IDH*^{wt} GBM STS. However, it is important to note that tapasin is part of the MHCI complex[45], and other factors may be involved in the efficiency of antigen presentation, especially in the context of the TME.

We also observed the overexpression of the immune checkpoint gene *CD274* (PD-L1) in *IDH*^{wt} GBM STS. A systematic study including more than 800 GBM samples from nine different studies also showed that PD-L1 expression in tumor tissues was associated with poor OS.[46] Patients with high CD274 levels should benefit from immunotherapies using anti-PD-L1 antibodies.[46]

Importantly, we also identified a 12-gene signature associated with *IDH*^{wt} GBM outcome. Using the LASSO regression with proportional hazards model, we could stratify *IDH*^{wt} GBM into high-risk and low-risk groups. This approach must be validated in other *IDH*^{wt} GBM NanoString cohorts, and if data support, it could be applied routinely for patient prognostication.

The present study exhibited some limitations. It only evaluated gene expression levels and analyzed a limited number of immune-related genes. Moreover, the number of cases assessing the genes differentially expressed between GBM IDHwt STS and LTS was limited. So, further studies addressing protein levels, the crosstalk among cell types, and functional studies should be performed. Also, studies evaluating a higher number of cases that would consider all the variables that influence patient survival, such as degree of surgery resection, age, and *MGMT* status, should be conducted to confirm the independent prognostic factor of our gene signature. Nevertheless, this study is of significant value since it was done using the nCounter technology, which allows routine FFPE archival material and could be easily reproduced in our series.[9] Finally, among the 24 differentially expressed genes identified in our series, 18 were also associated with GBM survival in the TCGA dataset. So, we believe that our results are consistent and important in understanding the role of immune-related genes in GBM biology.

Conclusions

We found that upregulation of immune-related genes, increased macrophage functions, and angiogenic factors are associated with poorer outcomes in *IDH*^{wt} GBM. Moreover, an immune-related gene expression signature could predict patient prognosis. Our findings identify several specific immune-related factors which may be associated with a more aggressive phenotype in GBM and provide promising and new unexplored targets for therapy.

Declarations

Ethics approval and consent to participate

This retrospective study was approved by the institutional review board from Barretos Cancer Hospital (IRB 1604/2018).

Consent for publication
Not applicable.

Author contribution(s)
Daniel Antunes Moreno: Conceptualization; Data curation; Formal analysis; Investigation; Methodology; Writing – original draft; Writing – review & editing.

Luciane Sussuchi da Silva: Data curation; Formal analysis; Investigation; Methodology; Writing – review & editing.

Isabella Gomes: Data curation; Writing – review & editing.

Letícia Ferro Leal: Investigation; Methodology; Writing – review & editing.

Gustavo Noriz Berardinelli: Methodology; Writing – review & editing.

Gisele Melo Gonçalves: Data curation; Writing – review & editing.

Caio Augusto Pereira: Data curation; Writing – review & editing.

Iara Viana Vidigal Santana: Data curation; Investigation; Writing – review & editing.

Marcus de Medeiros Matsushita: Data curation; Writing – review & editing.

Krishna Bhat: Investigation; Writing – review & editing.

Sean Lawler: Conceptualization; Investigation; Supervision; Writing – review & editing.

Rui Manuel Reis: Conceptualization; Funding acquisition; Investigation; Project administration; Supervision; Writing – review & editing.

Acknowledgements
Not applicable.

Funding
The authors disclosed receipt of the following financial support for the research, authorship, and/or publication of this article: Barretos Cancer Hospital and the Public Ministry of Labor Campinas (Research, Prevention, and Education of Occupational Cancer, Brazil). IG received a fellowship from São Paulo Research Foundation (FAPESP, 2018/10511-6). LFL and LSS received a fellowship from the Public Ministry of Labor Campinas (Research, Prevention, and Education of Occupational Cancer) in Campinas, Brazil. RMR is a recipient of a CNPq Productivity, Brazil. DM received a fellowship from National Oncology Care Support Program (PRONON), Brazil, and by a Technical Fellowship Award from the Union for International Cancer Control (UICC), 2020 for partnership with Brown University – Providence, RI, USA.

Competing interests
The authors declare that there is no conflict of interest.

Availability of data and materials
The datasets used and/or analyzed during the current study available from the corresponding author on reasonable request.

ORCID iD
Rui Manuel Reis https://orcid.org/0000-0002-9639-7940

Supplemental material
Supplemental material for this article is available online.

References

1. Ostrom QT, Cioffi G, Gittleman H, *et al.* CBTRUS statistical report: primary brain and other central nervous system tumors diagnosed in the United States in 2012-2016. *Neuro Oncol* 2019; 21: v1–v100.
2. Louis DN, Perry A, Wesseling P, *et al.* The 2021 WHO classification of tumors of the central nervous system: a summary. *Neuro Oncol* 2021; 23: 1231–1251.
3. Louis DN, Perry A, Reifenberger G, *et al.* The 2016 World Health Organization classification of tumors of the central nervous system: a summary. *Acta Neuropathol* 2016; 131: 803–820.
4. Verhaak RGW, Hoadley KA, Purdom E, *et al.* Integrated genomic analysis identifies clinically relevant subtypes of glioblastoma characterized by abnormalities in PDGFRA, IDH1, EGFR, and NF1. *Cancer Cell* 2010; 17: 98–110.
5. Wen PY and Reardon DA. Neuro-oncology in 2015: Progress in glioma diagnosis, classification and treatment. *Nat Rev Neurol* 2016; 12: 2015–2016.
6. Stupp R, Mason WP, van den Bent MJ, *et al.* Radiotherapy plus concomitant and adjuvant temozolomide for glioblastoma. *N Engl J Med* 2005; 352: 987–996.

7. Stupp R, Taillibert S, Kanner A, *et al.* Effect of tumor-treating fields plus maintenance temozolomide vs maintenance temozolomide alone on survival in patients with glioblastoma: a randomized clinical trial. *JAMA* 2017; 318: 2306–2316.

8. Paolillo M, Boselli C and Schinelli S. Glioblastoma under siege: an overview of current therapeutic strategies. *Brain Sci* 2018; 8: 15.

9. Gomes I, Moreno DA, dos Reis MB, *et al.* Low MGMT digital expression is associated with a better outcome of IDH1 wildtype glioblastomas treated with temozolomide. *J Neurooncol* 2021; 151: 135–144.

10. Sampson JH, Gunn MD, Fecci PE, *et al.* Brain immunology and immunotherapy in brain tumours. *Nat Rev Cancer* 2020; 20: 12–25.

11. Chen Z, Feng X, Herting CJ, *et al.* Cellular and molecular identity of tumor-associated macrophages in glioblastoma. *Cancer Res* 2017; 77: 2266–2278.

12. Berardinelli GN, Scapulatempo-Neto C, Durães R, *et al.* Advantage of HSP110 (T17) marker inclusion for microsatellite instability (MSI) detection in colorectal cancer patients. *Oncotarget* 2018; 9: 28691–28701.

13. Campanella NC, Berardinelli GN, Scapulatempo-Neto C, *et al.* Optimization of a pentaplex panel for MSI analysis without control DNA in a Brazilian population: correlation with ancestry markers. *Eur J Hum Genet* 2014; 22: 875–880.

14. Cesano A. nCounter® PanCancer immune profiling panel (NanoString Technologies, Inc., Seattle, WA). *J Immunother Cancer* 2015; 3: 42.

15. Simon N, Friedman J, Hastie T, *et al.* Regularization paths for Cox's proportional hazards model via coordinate descent. *J Stat Softw* 2011; 39: 1–13.

16. Viana-Pereira M, Lee A, Popov S, *et al.* Microsatellite instability in pediatric high grade glioma is associated with genomic profile and differential target gene inactivation. *PLoS One*; 6. Epub ahead of print 2011. DOI: 10.1371/journal.pone.0020588.

17. Bozdag S, Li A, Baysan M, *et al.* Master regulators, regulatory networks, and pathways of glioblastoma subtypes. *Cancer Inform* 2014; 13: 33–44.

18. Cohen AL, Holmen SL and Colman H. IDH1 and IDH2 mutations in gliomas. *Curr Neurol Neurosci Rep* 2013; 13: 345.

19. Zha C, Meng X, Li L, *et al.* Neutrophil extracellular traps mediate the crosstalk between glioma progression and the tumor microenvironment via the HMGB1/RAGE/IL-8 axis. *Cancer Biol Med* 2020; 17: 154–168.

20. Peñuelas S, Anido J, Prieto-Sánchez RM, *et al.* TGF-β increases glioma-initiating cell self-renewal through the induction of LIF in human glioblastoma. *Cancer Cell* 2009; 15: 315–327.

21. Poon CC, Gordon PMK, Liu K, *et al.* Differential microglia and macrophage profiles in human IDH-mutant and-wild type glioblastoma. *Oncotarget* 2019; 10: 3129–3143.

22. Sun L, Zhou H, Zhu Z, *et al.* Ex vivo and in vitro effect of serum amyloid a in the induction of macrophage M2 markers and efferocytosis of apoptotic neutrophils. *J Immunol* 2015; 194: 4891–4900.

23. Li Y, Cai L, Wang H, *et al.* Pleiotropic regulation of macrophage polarization and tumorigenesis by formyl peptide receptor-2. *Oncogene* 2011; 30: 3887–3899.

24. Xu Y, Geng R, Yuan F, *et al.* Identification of differentially expressed key genes between glioblastoma and low-grade glioma by bioinformatics analysis. *PeerJ* 2019. Epub ahead of print 2019. DOI: 10.7717/peerj.6560.

25. Georgoudaki AM, Prokopec KE, Boura VF, *et al.* Reprogramming tumor-associated macrophages by antibody targeting inhibits cancer progression and metastasis. *Cell Rep* 2016; 15: 2000–2011.

26. Sa JK, Chang N, Lee HW, *et al.* Transcriptional regulatory networks of tumor-associated macrophages that drive malignancy in mesenchymal glioblastoma. *Genome Biol* 2020; 21: 216.

27. Tong L, Li J, Choi J, *et al.* CLEC5A expressed on myeloid cells as a M2 biomarker relates to immunosuppression and decreased survival in patients with glioma. *Cancer Gene Ther* 2020; 27: 669–679.

28. Fei Y, Xiong Y, Shen X, *et al.* Cathepsin L promotes ionizing radiation-induced U251 glioma cell migration and invasion through regulating the GSK-3β/CUX1 pathway. *Cell Signal* 2018; 44: 62–71.

29. Gemmati D, Vigliano M, Burini F, *et al.* Coagulation factor XIIIA (F13A1): novel perspectives in treatment and pharmacogenetics. *Curr Pharm Des* 2016; 22: 1449–1459.

30. Porrello A, Leslie PL, Harrison EB, *et al.* Factor XIIIA-expressing inflammatory monocytes promote lung squamous cancer through fibrin cross-linking. *Nat Commun* 2018; 9: 1988.

31. Nold-Petry CA, Rudloff I, Baumer Y, *et al*. IL-32 promotes angiogenesis. *J Immunol* 2014; 192: 589–602.
32. Lui AJ, Geanes ES, Ogony J, *et al*. IFITM1 suppression blocks proliferation and invasion of aromatase inhibitor-resistant breast cancer in vivo by JAK/STAT-mediated induction of p21. *Cancer Lett* 2017; 399: 29–43.
33. Hsu YY, Shi GY, Wang KC, *et al*. Thrombomodulin promotes focal adhesion kinase activation and contributes to angiogenesis by binding to fibronectin. *Oncotarget* 2016; 7: 68122–68139.
34. Seon BK, Haba A, Matsuno F, *et al*. Endoglin-targeted cancer therapy. *Curr Drug Deliv* 2010; 8: 135–143.
35. Dieterich LC, Mellberg S, Langenkamp E, *et al*. Transcriptional profiling of human glioblastoma vessels indicates a key role of VEGF-A and TGFβ2 in vascular abnormalization. *J Pathol* 2012; 228: 378–390.
36. Long S, Li M, Liu J, *et al*. Identification of immunologic subtype and prognosis of GBM based on TNFSF14 and immune checkpoint gene expression profiling. *Aging* 2020; 12: 7112–7128.
37. Ruano Y, Mollejo M, Ribalta T, *et al*. Identification of novel candidate target genes in amplicons of Glioblastoma multiforme tumors detected by expression and CGH microarray profiling. *Mol Cancer* 2006; 5: 39.
38. Gielen PR, Schulte BM, Kers-Rebel ED, *et al*. Elevated levels of polymorphonuclear myeloid-derived suppressor cells in patients with glioblastoma highly express S100A8/9 and arginase and suppress T cell function. *Neuro-Oncol* 2016; 18: 1253–1264.
39. Zhang X, Chen L, Dang W qi, *et al*. CCL8 secreted by tumor-associated macrophages promotes invasion and stemness of glioblastoma cells via ERK1/2 signaling. *Lab Invest* 2020; 100: 619–629.
40. Bouwens van der Vlis TAM, Kros JM, Mustafa DAM, *et al*. The complement system in glioblastoma multiforme. *Acta neuropathol commun* 2018; 6: 91.
41. Lubbers R, van Essen MF, van Kooten C, *et al*. Production of complement components by cells of the immune system. *Clin Exp Immunol* 2017; 188: 183–194.
42. Luckheeram RV, Zhou R, Verma AD, *et al*. CD4 +T cells: differentiation and functions. *Clin Dev Immunol* 2012. Epub ahead to print March 2012. DOI: 10.1155/2012/925135.
43. Conrad C, Gregorio J, Wang YH, *et al*. Plasmacytoid dendritic cells promote immunosuppression in ovarian cancer via ICOS costimulation of Foxp3+ T-regulatory cells. *Cancer Res* 2012; 72: 5240–5249.
44. Iwata R, Hyoung Lee J, Hayashi M, *et al*. ICOSLG-mediated regulatory T-cell expansion and IL-10 production promote progression of glioblastoma. *Neuro Oncol* 2020; 22: 333–344.
45. Fisette O, Wingbermühle S, Tampé R, *et al*. Molecular mechanism of peptide editing in the tapasin-MHC I complex. *Sci Rep* 2016; 6: 1–13.
46. Hao C, Chen G, Zhao H, *et al*. PD-L1 expression in glioblastoma, the clinical and prognostic significance: a systematic literature review and meta-analysis. *Front Oncol* 2020; 10: 1015.